absorbable adhesion barrier: a prospective randomized multicenter clinical study. Feritil Steril 1989;51:933–8.
[5] Burns JW, Skinner K, Colt J, Sheidlin A, Bronson R, Yaacobi Y, Goldberg EP. Prevention of tissue injury and postsurgical adhesions by precoating tissues with hyaluronic acid solutions. J Surg Res 1995;59:644–52.
[6] Campoccia D, Doherty P, Radice M, Brun P, Abatangelo G, Williams DF. Semisynthetic resorbable materials from hyaluronan esterification. Biomaterials 1998;19:2101–27.
[7] Spotniz WD. History of tissue adhesives. In: Sierra D, Saits R, editors. Surgical adhesives and sealants, current technology and applications. USA: Technomic; 1996. p. 3–11.
[8] Tseng YC, Hyon SH, Ikada Y, Shimizu Y, Tamura K, Hitomi S. In vivo evaluation of 2-cyanoacrylates as surgical adhesives. J Appl Biomater 1990;1:111–9.
[9] Matsuda T, Nakajima N, Itoh T, Takakura T. Development of a compliant surgical adhesive derived from novel fluorinated hexamethylene diisocyanate. ASAIO 1989;35:381–3.
[10] Ohya S, Nakayama Y, Matsuda T. Thermoresponsive artificial extracellular matrix for tissue engineering: hyaluronic acid bioconjugated with poly(*N*-isopropylacrylamide) grafts. Biomacromolecules 2001;2:856–63.
[11] Ohya S, Nakayama Y, Matsuda T. Artificial extracellular matrix design in tissue engineering: synthesis of thermoresponsive hyaluronic acid and its supramolecular organization. Jpn J Artif Organs 2000;29:446–51.
[12] Morikawa N, Matsuda T. Thermoresponsive artificial extracellular matrix: *N*-isopropylacrylamide-graft-copolymerized gelatin. J Biomater Sci, Polym Ed 2002;13:167–83.
[13] Matsuda T. Molecular design of functional artificial extracellular matrix: thermoresponsive gelatin. Jpn J Artif Organs 1999;28:242–5.
[14] Ohya S, Nakayama Y, Matsuda T. Material design for artificial extracellular matrix: cell entrapment in poly(*N*-isopropylacrylamide) (PNIPAM)-grafted gelatin hydrogel. J Artif Organs 2001;4:308–14.

TISSUE ENGINEERING
Volume 10, Number 11/12, 2004

Novel Strategy for Soft Tissue Augmentation Based on Transplantation of Fragmented Omentum and Preadipocytes

TEIICHI MASUDA, M.D.,[1,2] MASUTAKA FURUE, M.D., Ph.D.,[2] and TAKEHISA MATSUDA, Ph.D.[1]

ABSTRACT

Current therapeutic procedures for soft tissue augmentation still lack the ability to induce rapidly formation of adipose tissue and its long-term stability, which is determined by rapid revascularization. The omentum is highly vascularized with microvascular endothelial cells (ECs) and is composed mainly of adipocytes that produce an enormously high level of vascular endothelial growth factor (VEGF). The aim of this study was to determine the potential usefulness of fragmented omentum tissues, with or without cotransplantation with preadipocytes, in soft tissue augmentation. Fragmented omentum tissues (approximately 500 mg) with or without preadipocytes (approximately 2.3×10^6) isolated from epididymal adipose tissues were transplanted under the dorsal skin of Wistar rats by percutaneous injection and the tissues were left under the skin for up to 12 weeks. Regardless of cotransplantation with preadipocytes, the general morphological features of the transplanted tissue were as follows. The transplanted tissues, the weight loss of which was limited to 30–40%, contained viable adipocytes and some pseudocysts surrounded by fibrotic septa with minor inflammatory cell infiltration. High levels of triacylglycerol content, capillary density, and VEGF production were observed in transplanted tissues 12 weeks postoperation. Cotransplantation with preadipocytes enhanced adipose tissue formation significantly. These observations strongly indicate that transplantation of fragmented omentum tissues or cotransplantation with preadipocytes may be a promising therapeutic procedure for soft tissue augmentation.

INTRODUCTION

DESPITE MANY YEARS OF EFFORT, various attempts, and clinical trials and practices, the reconstruction of soft tissue defects is still unsatisfactory in outcome and presents unsolved problems. Therapeutic procedures for soft tissue augmentation are classified into three approaches (each of which has inherent problems). One approach is the autologous transplantation of adipose tissues or adipocyte-rich tissues, which are harvested by suction or surgical excision.[1–8] The subcutaneous injection of suctioned adipose tissue, which gained popularity with the growing prevalence of liposuction techniques, resulted in continuous volumetric reduction with time, probably due to combined reasons such as the reduced viability of adipocytes as a result of suctioning, the low tolerance of adipocytes to ischemia, and the slow revascularization of transplanted tissue.[7,8] The second approach is the injection of a liquid synthetic polymer (silicone) or biomacromolecule-containing solution (collagen or hyaluronic acid).[9,10] The former has been abandoned because of toxicological problems and the latter has the shortcoming of fast volumetric loss due to rapid degradation and sorption. The latest approach is soft tissue augmen-

[1]Division of Biomedical Engineering, and [2]Department of Dermatology, Graduate School of Medical Sciences, Kyushu University, Fukuoka, Japan.

tation by tissue engineering: preadipocyte–polymer matrix constructs are inserted subcutaneously[11–16] or *in situ* adipose tissue formation is observed via the slow release of angiogenic factors or differentiating factors from implanted matrices.[16–20] The major shortcoming of this approach is retarded volumetric gain due to slow vascularization.

From the above-mentioned problems, it may be concluded that the requirements for soft tissue augmentation are (1) rapid volumetric gain to fill defects and (2) continuous maintenance of adipose tissue without time-dependent volumetric loss. It is strongly conceived that the rapid revascularization of transplanted adipose tissue is a crucial factor for the success of adipose tissue transplantation.

The omentum is a large plica of the mobile peritoneum, is highly vascularized, and is filled with adipose tissue.[21] In addition to the enormous number of microvascular endothelial cells (ECs)[22] in its tissue, the omentum has a high vascularization capacity,[23] which has been proven by the fact that the omentum is used as a pedicle graft for brain,[24] heart,[25] and lower extremity revascularization.[26] One study revealed that among various cell types in the body, adipocytes in the omentum are characterized by the highest production of vascular endothelial growth factor (VEGF), a major angiogenic factor.[27]

The omentum has been used for soft tissue augmentation of breasts and facial contour defects as a pedicle flap or a free flap, using microvascular anastomosis, and cosmetic results were reported satisfactory.[28–31] The usefulness of free omental grafts in soft tissue augmentation, however, has not been fully evaluated. Almost two decades ago, a preliminary report on the experimental study of free omental grafts (without fragmentation) showed that a considerable volumetric gain was achieved in the early phase of transplantation but ischemic necrosis at the central area of the transplanted tissue was noted.[32] No further study was reported despite promising results.

In this article, to overcome the problems mentioned above and to maximally utilize the inherent nature of omentum tissues, fragmented or minced omentum tissues were subcutaneously injected, and the time-dependent changes in tissue morphogenesis were examined: at the tissue, cellular, and genetic levels. The advantage of injection is that it enables the transplantation of tissue without major scarring, which is inevitable when tissue transplantation was performed by surgical procedures. Preadipocytes were expected to contribute to regenerate adipose tissue.

The results of this study were compared with those of the cotransplantation of fragmented omentum tissues with preadipocytes. The potential usefulness of fragmented omentum tissue in soft tissue augmentation in clinical settings is discussed.

MATERIALS AND METHODS

Materials

Collagenase (type II), dexamethasone, isobutyl methylxanthine (IBMX), and 3,3-diaminobenzidine were purchased from Sigma (St. Louis, MO). Anti-human von Willebrand factor (vWF) antibody, anti-rat proliferating cell nuclear antigen (PCNA) antibody, and peroxidase-conjugated IgG antibody were purchased from Dako-Cytomation (Carpinteria, CA). All other reagents were purchased from Wako Pure Chemical Industries (Osaka, Japan).

Isolation and culture of rat preadipocytes

Animal experiments were reviewed by the Committee of Ethics on Animal Experimentation of the Faculty of Medicine, Kyushu University (Fukuoka, Japan) and carried out in accordance with the *Guidelines for Animal Experiments* of the Faculty of Medicine, Kyushu University and the Law (No. 105) and Notification (No. 6) of the Japanese Government. Six-week-old male Wistar rats weighing 200 to 250 g (Kyudou, Saga, Japan) were anesthetized by intraperitoneal injection of pentobarbital sodium (40 mg/kg). Epididymal adipose tissues were aseptically harvested and placed in a 4°C saline solution supplemented with penicillin (500 U/mL) and streptomycin (500 μg/mL). The harvested tissues were enzymatically digested in Dulbecco's modified Eagle's medium (DMEM) supplemented with 0.05% (w/v) type II collagenase and 5% (w/v) bovine serum albumin for 30 min at 37°C on a shaker. The digested tissues were filtered through a 250-μm pore size sieve and then through a 100-μm pore size filter to separate undigested debris and capillary fragments from preadipocytes. The filtered cell suspension was centrifuged and the resulting pellet of preadipocytes was then plated at 10^4 cells/cm^2 onto plastic culture dishes in DMEM supplemented with 10% fetal bovine serum (FBS), penicillin (100 U/mL), and streptomycin (100 μg/mL). During cell expansion, the preadipocytes were subcultured before confluency because contact inhibition initiates adipocyte differentiation and stops preadipocyte proliferation. The cells were expanded two times and subjected to *in vivo* experiments. The differentiation of preadipocytes into adipocytes was accomplished by culturing confluent monolayers of cells in DMEM with 10% FBS, penicillin (100 U/mL), streptomycin (100 μg/mL), insulin (10 mg/mL), 1 mM dexamethasone, 0.5 mM IBMX, and 200 mM indomethacin for 72 h. The medium was then withdrawn and replaced with DMEM with 10% FBS, penicillin (100 U/mL), streptomycin (100 μg/mL), and insulin (5 mg/mL) and the cell culture was continued. On day 7, Sudan II staining of cultured cells was performed and the morphological assessment of differentiation was microscopically

quantified by counting cells containing visible lipid droplets.[33,34] For each sample, five different fields were examined and the percentage of lipid-containing cells was determined with an optical microscope (TE300, Nikon, Tokyo, Japan) at ×200 magnification.

In vivo *experiments*

Thirty Wistar rats weighing 330 to 380 g were used. Rats were distributed to two experimental groups.

Group I: In 15 rats, the greater omentum was removed through a midline incision. After the omentum was fragmented into 1-2-mm^3 sizes with a scalpel, the fragments were washed twice with physiological saline and were mixed with preadipocytes previously isolated and cultured from the same rat according to the methods described above. The mixture of omentum fragments and preadipocytes harvested from the same rat was injected between the rat's dorsal skin and the underlying muscle by percutaneous injection (18-gauge needle with 1-mL syringe). The mean weight of the injected omentum fragments was 524.5 ± 42.8 mg and the mean number of injected preadipocytes was $(2.3 \pm 1.4) \times 10^6$.

Group II: Another set of 15 rats received an injection of omentum fragments in between the dorsal skin and the underlying muscle by percutaneous injection. The mean weight of the injected omentum fragments was 501.2 ± 55.4 mg.

The rats were killed with an overdose of intraperitoneal pentobarbital sodium (200 mg/kg body weight) 2, 4, or 12 weeks postoperation (five rats for each group, for each transplantation period). The transplanted tissues were removed and weighed for comparison of their weight with that at the time of transplantation. After the sample was weighed, half of the sample was fixed in 10% formalin and then embedded in paraffin and sectioned for hematoxylin and eosin (H&E) staining, and further immunohistochemical studies. The residual half was divided in two pieces; one was used for triacylglycerol (TG) content measurement and the other was kept frozen (−80°C) for reverse transcription-polymerase chain reaction (RT-PCR) and enzyme immunoassay studies.

Immunohistochemical studies

Deparaffinized cross-sections (4 μm thick) were incubated with antibodies to human vWF (1:1600 dilution) and rat PCNA (1:200 dilution) at 4°C for 16 h. After further incubation with a peroxidase-conjugated secondary antibody, peroxidase activity was visualized with 3,3′-diaminobenzidine. The immunostained sections were counterstained with hematoxylin. Ten different fields were selected for determining the number of capillaries and PCNA-positive cells under an optical microscope (TE300, ×200 magnification; Nikon).

In situ *labeling of apoptotic cells*

Apoptotic cells were visualized by the terminal deoxynucleotidetransferase-mediated deoxyuridine triphosphate (dUTP) nick end-labeling (TUNEL) method, using a commercially available *in situ* apoptosis detection kit (Takara *in situ* apoptosis detection kit; Takara Bio, Shiga, Japan). The sections were counterstained with hematoxylin. Ten different fields were selected for determining the number of apoptotic cells under an optical microscope (×200 magnification).

Triacylglycerol content

The TG content of each sample was determined as described previously.[20] Briefly, total lipid was extracted with chloroform–methanol (1:2) and TG content was measured with a triglyceride E-test kit (Wako Pure Chemical Industries) according to the manufacturer's instructions.

Reverse transcription-polymerase chain reaction

Total RNA was obtained from approximately 50 mg of the harvested samples using ISOGEN (Nippon Gene, Tokyo, Japan) according to the manufacturer's instruction. With a commercially available kit (Ready-to-Go T-primed first-strand kit; Amersham Biosciences, Piscataway, NJ), 3.5 μg of total RNA was reverse transcribed to cDNA and amplified by PCR. The primers used for the detection of VEGF mRNA were 5′-CCGAATTCACCAAAGAAAGATAGAACAAAG (sense) and 5′-GGTGAGAGGTCTAGTTCCCGA (antisense).[35] The PCR was performed under the following conditions: denaturation at 98°C for 2 min followed by 5 cycles of 30 s at 98°C, 30 s at 48°C, and 30 s at 72°C (first step); 30 cycles of 30 s at 98°C, 30 s at 57°C, and 30 s at 72°C (second step). The samples were then treated at 72°C for 7 min. The primers used in the detection of basic fibroblast growth factor (bFGF) mRNA were 5′-GCCTTCCCACCCGGCCACTTCAAGG (sense) and 5′-GCACACACTCCCTTGATGGACACAA (antisense).[36] The thermal cycler conditions consisted of 2 min of denaturation at 96°C followed by 35 cycles of 30 s at 96°C, 30 s at 60°C, and 30 s at 72°C. The samples were then treated at 72°C for 7 min. The primers used for the detection of hepatocyte growth factor (HGF) mRNA were 5′-GGGGAATGAAATGCAGTCAG (sense) and 5′-CCTGTATCCATGGATGCTTC (antisense).[37] The thermal cycler conditions consisted of 2 min of denaturation at 96°C followed by 30 cycles of 30 s at 96°C, 30 s at 56°C, and 30 s at 72°C. The samples were then treated at 72°C for 7 min. The primers used for the detection of glyceraldehyde-3-phosphate dehydrogenase (GAPDH) mRNA as a

positive control were 5'-ACCACAGTCCATGCCATCAC (sense) and 5'-TCCACCACCCTGTTGCTGTA (antisense) (Toyobo, Osaka, Japan). The thermal cycler conditions consisted of 2 min of denaturation at 98°C followed by 30 cycles of 60 s at 98°C, 60 s at 56°C, and 60 s at 72°C. The samples were then treated at 72°C for 7 min. The RT-PCR products were analyzed by electrophoresis on 2% agarose gels. The sizes of the expected products were 311, 239, and 107 bp, depending on splicing form for the mRNA of VEGF ($VEGF_{188}$, 311 bp; $VEGF_{164}$, 239 bp; $VEGF_{120}$, 107 bp), 179 bp for mRNA of bFGF, 314 bp for mRNA of HGF, and 452 bp for mRNA of GAPDH.

Enzyme immunoassay

Total protein was obtained from approximately 50 mg of the harvested samples, using ISOGEN according to the manufacturer's instructions. To quantify the levels of VEGF, bFGF, and HGF in the tissue lysate, a commercially available enzyme immunoassay kit was used (VEGF [ACCUCYTE; CytImmune Sciences, College Park, MD]; bFGF [Quantikine; R&D Systems, Minneapolis, MN]; HGF [rat HGF EIA, Institute of Immunology, Tokyo, Japan]) according to the manufacturer's instructions. For value standardization, total protein concentration was measured with a commercially available protein assay kit (Bio-Rad protein assay; Bio-Rad Laboratories, Hercules, CA).

Statistical analysis

Experimental results were expressed as means ± standard deviation (SD). The data were subjected to statistical analysis, using analysis of variance (ANOVA). Statistical analysis was carried out by ANOVA with paired t test or Bonferroni/Dunn post hoc test; $p < 0.05$ was considered statistically significant. All statistical analyses were performed with StatView 5.0 (SAS Institute, Cary, NC).

RESULTS

Transplantation

Approximately 500 mg of fragmented omentum tissues or a mixture of fragmented tissues and preadipocyte-containing cells (approximately 2.3×10^6) was autologously transplanted under rat dorsal skin and adipose tissue morphogenesis was examined with transplantation time at the tissue, cellular, and mRNA levels. Group I received fragmented omentum tissues and preadipocyte-containing cells, and group II received only fragmented omentum tissues. The fragmented omentum tissues before transplantation were found to be composed of adipose tissues and a well-developed capillary network (Fig. 1A). As for preadipocytes, they were isolated from epididymal adipose tissues and cultured in medium containing differentiation agents (insulin, dexamethasone, isobutyl methylxanthine, and indomethacin). The intracellular accumulation of fat droplets was observed by Sudan II staining (Fig. 1B), indicating that some cells differentiated into adipocytes under the culture conditions mentioned above. Morphological assessment of differentiation revealed that 39.2 ± 11.2% ($n = 19$) of cultured cell contained lipid droplets, indicating that approximately 40% of the transplanted cells were preadipocytes.

Gross observation of the transplanted area showed that the mass of tissue at transplantation gradually decreased in size as transplantation proceeded, even at 12 weeks postoperation (Fig. 2). Table 1 lists the time-dependent changes in the weight of transplanted tissues harvested at 2, 4, and 12 weeks postoperation (each, $n = 5$). The

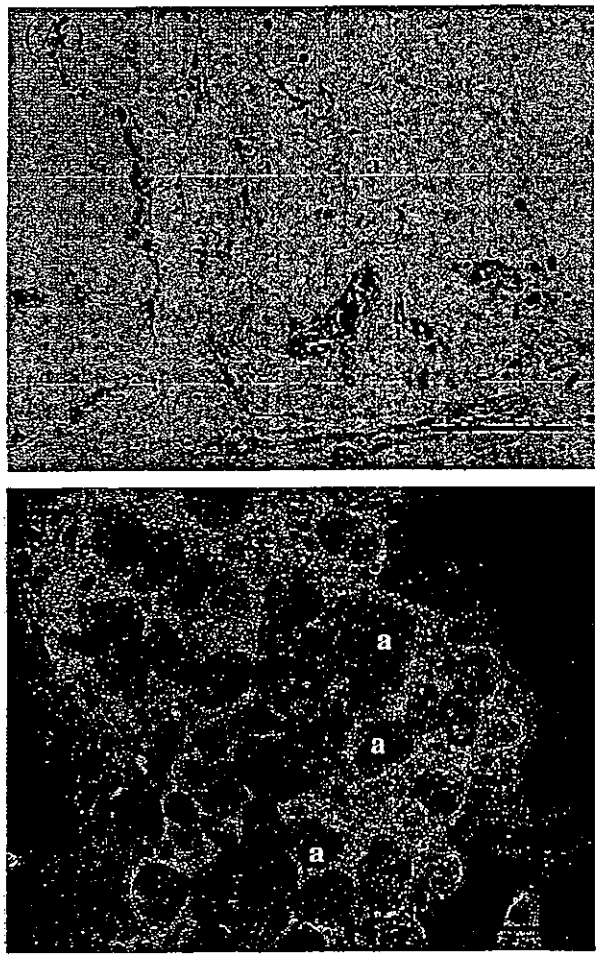

FIG. 1. (A) Omentum tissue (hematoxylin and eosin staining) composed of adipocytes (a) and well-developed capillary network (c). (B) Preadipocytes and differentiating adipocytes isolated from epididymal adipose tissue (Sudan II staining). Original magnification, ×200; scale bars, 100 μm.

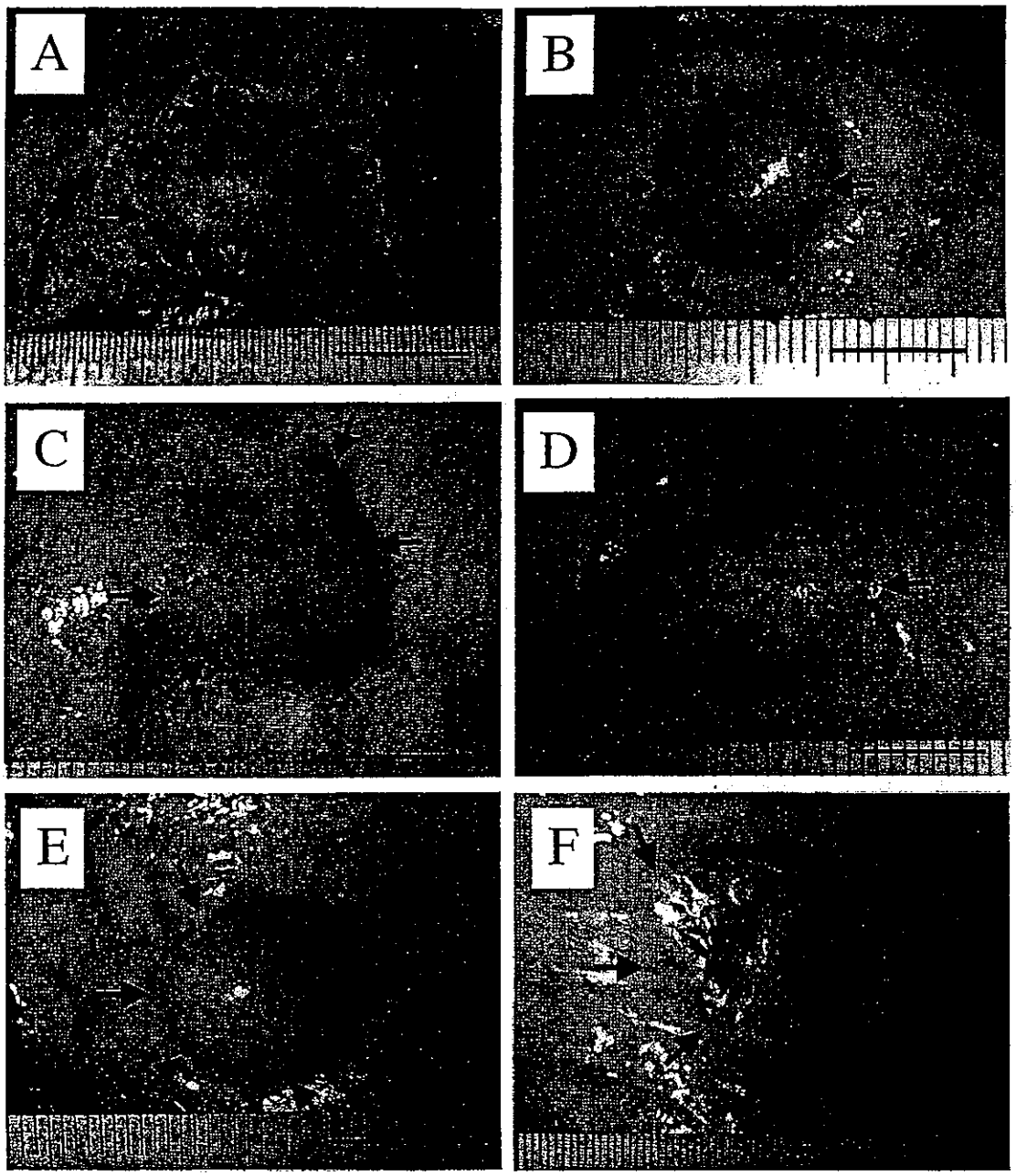

FIG. 2. Time-dependent changes in gross appearance of the transplanted area in group I [(A) 2 weeks postoperation; (B) 4 weeks postoperation; (C) 12 weeks postoperation] and group II [(D) 2 weeks postoperation; (E): 4 weeks postoperation; (F) 12 weeks postoperation]. Scale bars: 1 cm.

mean weights of harvested tissues were approximately 85% of the transplanted tissue at 2 weeks postoperation and 70% at 4 weeks postoperation, irrespective of the group. However, there were no significant time-dependent changes in the mean weights of transplanted tissues regardless of the group during these observation periods. At 12 weeks postoperation, the mean weights of tissues harvested decreased significantly to 60% of the transplanted tissues for group II ($p = 0.0072$), whereas there were no significant time-dependent changes in the mean weights of transplanted tissues in group I (mean, 71%).

Tissue morphology

Histological observations. Figures 3 and 4 show the H&E-stained sections of groups I and II at postoperative weeks 2 and 12. Irrespective of the group, the following general histological observations were made. At

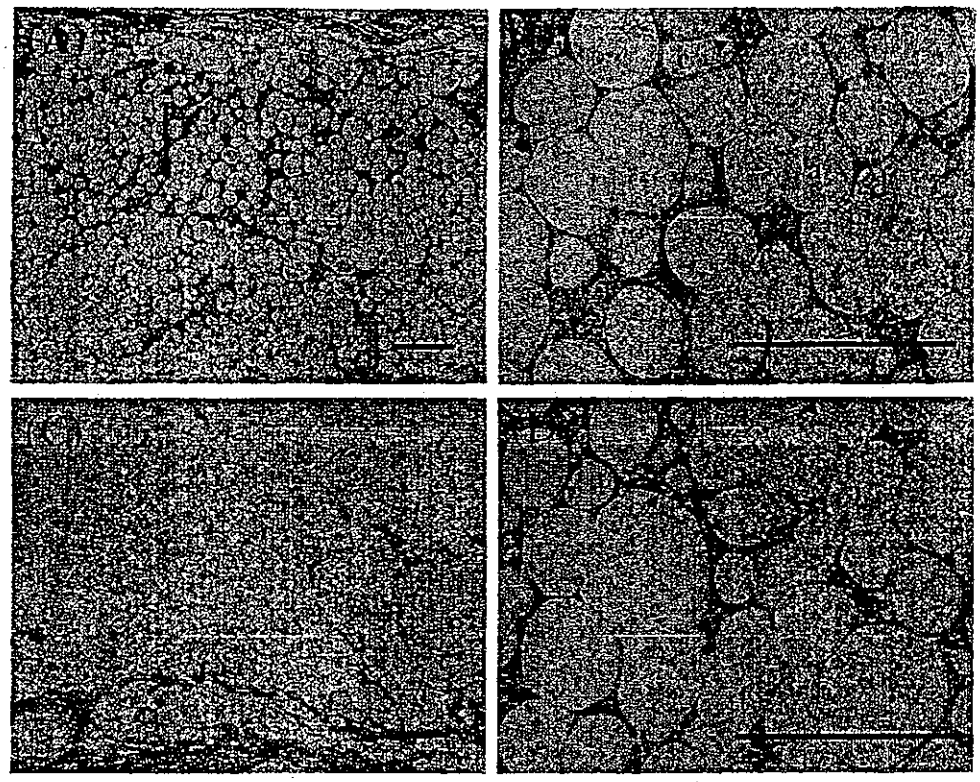

FIG. 3. Excised adiposed tissue after transplantation in group I [(A and B) 2 weeks postoperation; (C and D) 12 weeks postoperation]. a, adipocyte; c, capillary; f, fibrotic septa; p, pseudocyst. Hematoxylin and eosin staining. Original magnification: (A and C) ×40; (B and D) ×200. Scale bars: 200 μm.

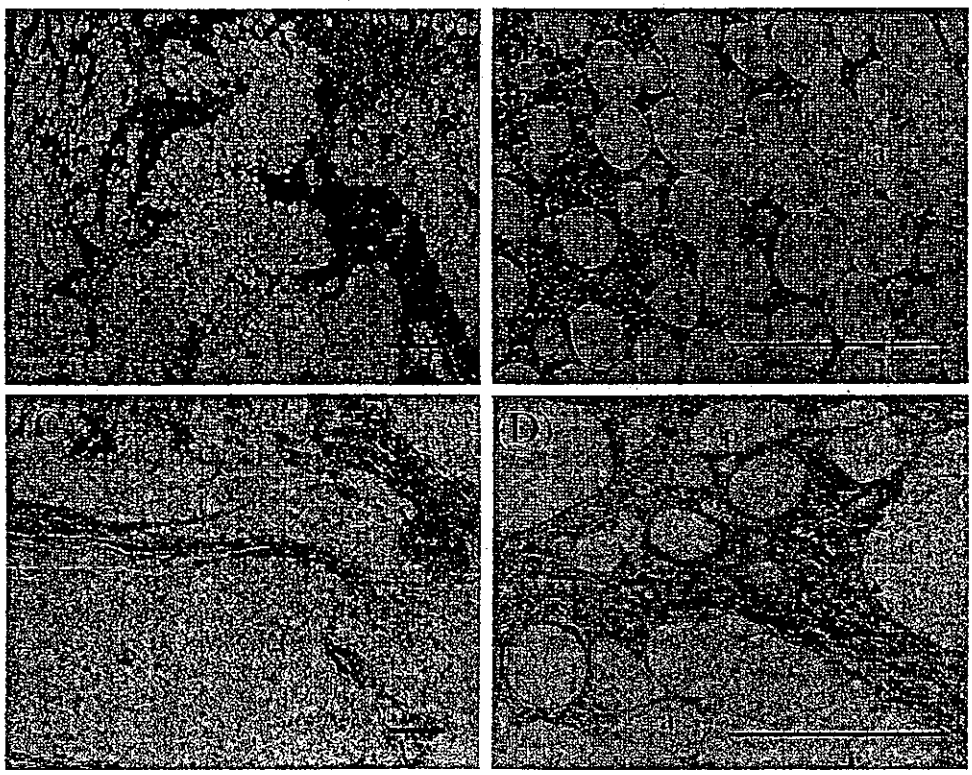

FIG. 4. Excised adiposed tissue after transplantation in group II [(A and B) 2 weeks postoperation; (C and D) 12 weeks postoperation]. a, adipocyte; c, capillary; f, fibrotic septa; p, pseudocyst. Hematoxylin and eosin staining. Original magnification: (A and C) ×40; (B and D) ×200. Scale bars: 200 μm.

2 weeks postoperation, an extensive infiltration of inflammatory cells into the viable fragmented omentum tissues was observed. The formation of pseudocysts, derived from the fusion of dead adipocytes, was observed around the area of cell infiltration (Fig. 3A and B and Fig. 4A and B). At 4 weeks postoperation, fibrosis became distinct between the viable fragmented omentum tissues and the infiltration of inflammatory cells around the viable adipocytes was markedly reduced (data not shown). At 12 weeks postoperation, the transplanted tissues were composed mainly of viable adipocytes and some pseudocysts surrounded by fibrotic septa with mild infiltration by inflammatory cells (Fig. 3C and D and Fig. 4C and D).

Capillary density. Immunohistochemical staining of von Willebrand factor (vWF) specific to endothelial cells was performed to determine the capillary densities of transplanted tissues. Capillary densities were found to be approximately 105 capillaries/mm^2 for omentum tissue, and 45 capillaries/mm^2 for the surrounding tissue to be transplanted. Capillary densities of transplanted tissues decreased significantly to approximately 60% of that of omentum tissue (approximately 65 capillaries/mm^2) at 2 weeks postoperation in groups I and II (group I, $p = 0.0006$; group II, $p = 0.0007$), but increased to the preoperation level at 4 weeks postoperative (Fig. 5). There was no significant difference in capillary density between groups I and II throughout the transplantation period. Capillary densities of the transplanted tissues in groups I and II were almost 1.5-fold to 2.5-fold higher than that of the surrounding tissue ($p = 0.001$–0.0066).

Proliferating and apoptotic cells. Immunohistochemical staining of proliferating cell antigen (PCNA) and the terminal deoxynucleotidetransferase-mediated deoxyuridine triphosphate (dUTP) nick end-labeling (TUNEL) method were used to determine the numbers of proliferating and apoptotic cells in transplanted tissues, respectively. The numbers of PCNA-positive cells were approximately 85 cells/mm^2 for the omentum tissue and 40 cells/mm^2 for the surrounding tissue to be transplanted. The numbers of TUNEL-positive cells were approximately 0.5 cell/mm^2 for the omentum tissue and 0.4 cell/mm^2 for the surrounding tissue to be transplanted. The numbers of PCNA-positive cells for the transplanted tissues at 2 and 4 weeks postoperation were almost 5-fold higher ($p = 0.0052$–0.0467) than for the omentum tissue or 10-fold higher ($p = 0.0052$–0.0252) than for the surrounding tissue (Fig. 6A). The numbers of TUNEL-positive cells for the transplanted tissues were almost 15-fold higher ($p = 0.0001$, group I; $p = 0.0003$, group II) at 2 weeks postoperation than for the omentum tissue in groups I and II (Fig. 6B). However, the numbers of PCNA-positive cells and apoptotic cells decreased considerably, approaching those of the surrounding tissues, at 12 weeks postoperation. There was no significant difference in the numbers of both PCNA- and TUNEL-positive cells between groups I and II throughout the transplantation period. Overall, the number of proliferating cells was almost 60- to 100-fold higher than that of apoptotic cells throughout the transplantation period.

Lipid accumulation

Triacylglycerol (TG) content, determined after extraction of total lipid from the transplanted tissues, was found to be approximately 560 mg/g for the omentum

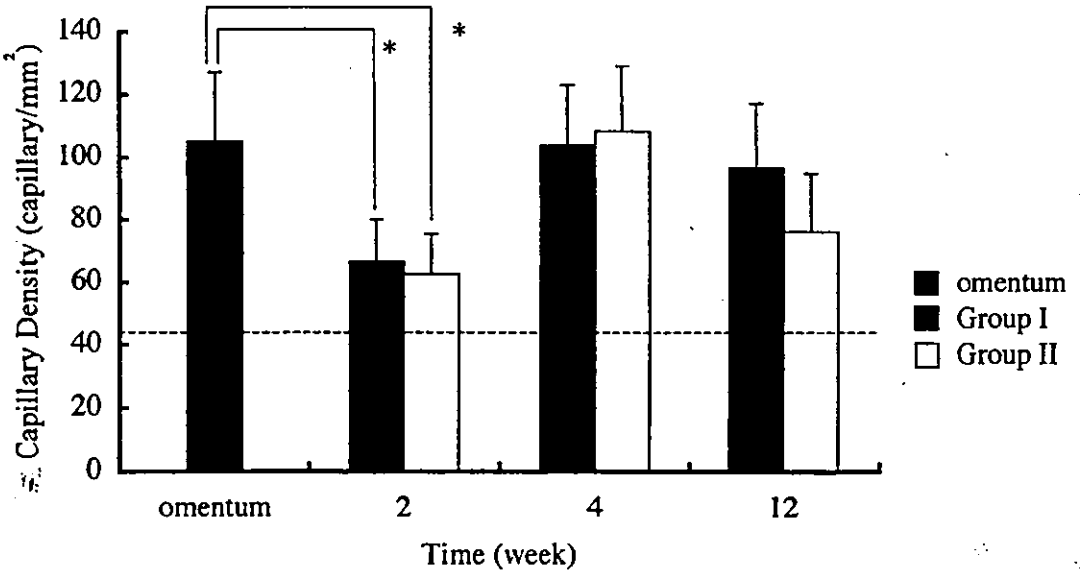

FIG. 5. Time-dependent changes in capillary densities of transplanted tissues (group I, solid columns; group II, open columns; each, $n = 5$). Dashed line indicates the capillary density of the surrounding subcutaneous tissue (42 capillaries/mm^2). Data represent means ± SD. *$p < 0.05$.

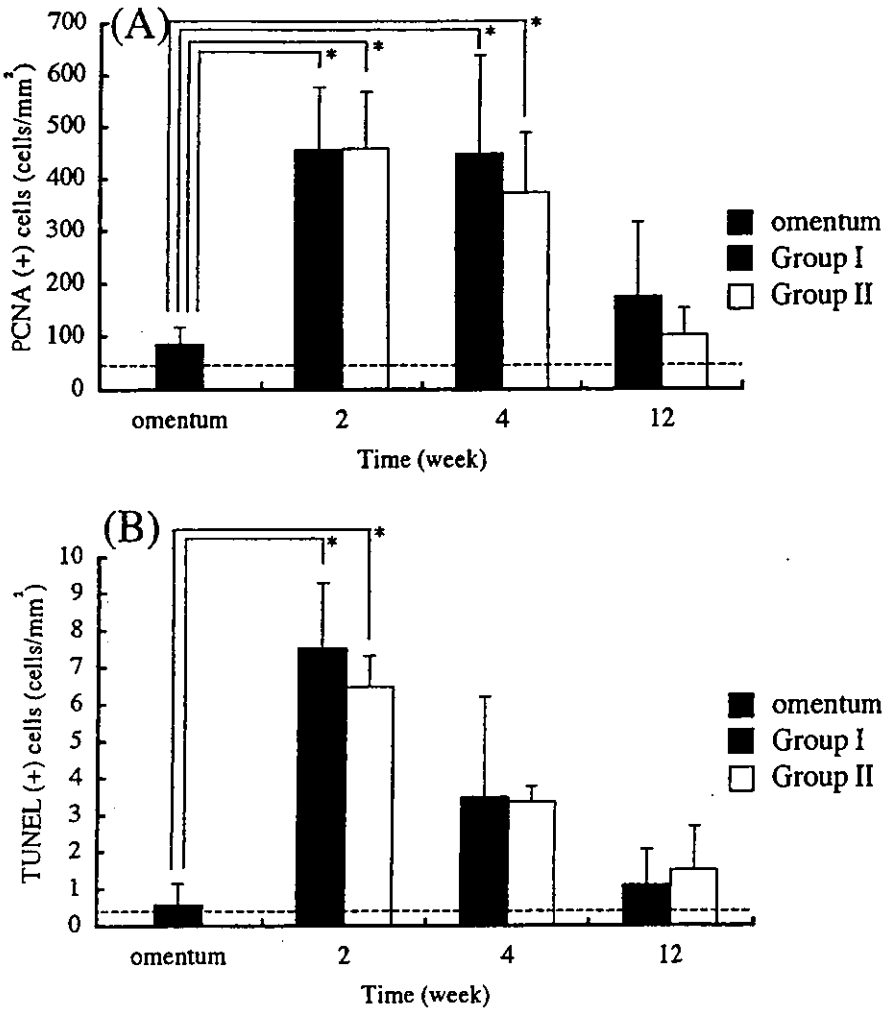

FIG. 6. Time-dependent changes in the numbers of PCNA-positive cells (A) and TUNEL-positive cells (B) of transplanted tissues (group I, solid columns; group II, open columns; each, $n = 5$). Dashed lines indicate the numbers of PCNA-positive cells (A, 42 cells/mm^2) and TUNEL-positive cells (B, 0.43 cell/mm^2) in the surrounding subcutaneous tissue. Data represent means ± SD. *$p < 0.05$.

tissue, and 17 mg/g for the surrounding tissue to be transplanted. In groups I and II, the TG content of transplanted tissues was almost one-half that of the omentum tissue at 2 and 4 weeks postoperation ($p = 0.0003$–0.0184). On the other hand, at 12 weeks postoperation, the TG content of transplanted tissues in group I increased to almost 75% of that of omentum tissue, but for group II it remained unchanged regardless of transplantation period (Fig. 7).

Growth factor expression and production

mRNA expression of three potent growth factors and angiogenic factors (HGF, bFGF, and VEGF) was determined by the RT-PCR technique. mRNA expression of HGF and bFGF was detected regardless of the transplantation period or group. As for VEGF, among the three isoforms, $VEGF_{164}$ (239 bp) and $VEGF_{120}$ (107 bp) had stronger mRNA signals and their continuous expression for both groups was observed throughout the transplantation period (Fig. 8).

The amount of VEGF, bFGF, and HGF produced in the transplanted tissues, determined by an enzyme immunoassay, showed that the amount of VEGF produced was approximately 4 ng/mg of protein in omentum tissue, and VEGF was not detected in the surrounding tissue to be transplanted. The amount of VEGF in the transplanted tissues produced ranged from 2.6 to 4.4 ng/mg of protein throughout the transplantation period (Fig. 9). There was no significant difference in terms of the amount of VEGF production throughout the transplantation period in groups I and II. bFGF and HGF protein was not detected (or was present at less than the detectable limit of enzyme immunoassay kits used) in the tissues regardless of the group or the transplantation period.

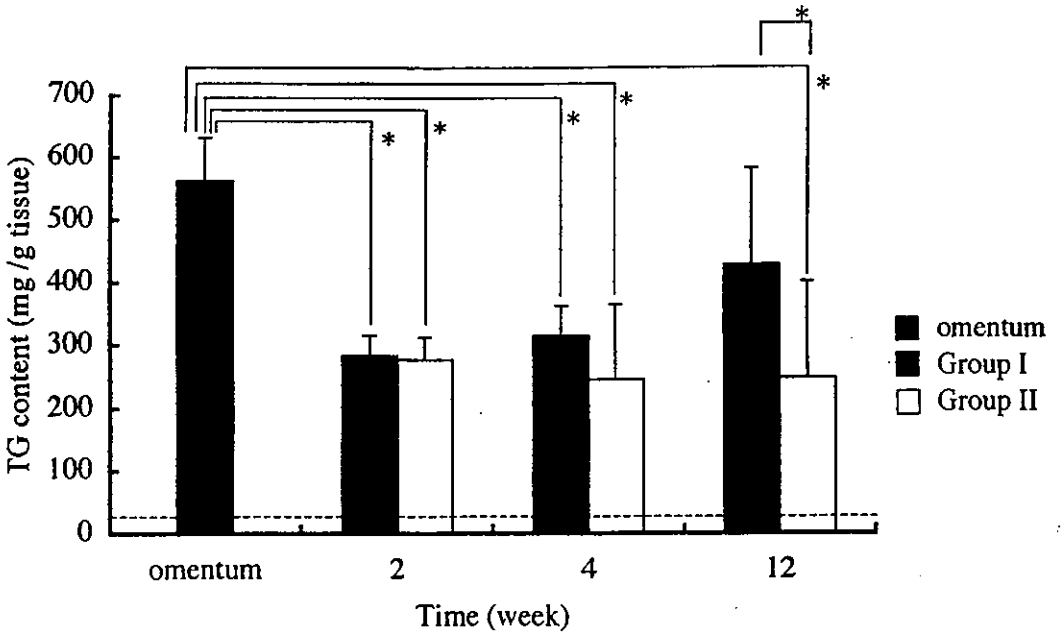

FIG. 7. Time-dependent changes in the triacylglycerol (TG) content of transplanted tissues (group I, solid columns; group II, open columns; each, $n = 5$). Dashed line indicates the triacylglycerol content of the surrounding subcutaneous tissue (17 mg/g tissue). Data represent means ± SD. $*p < 0.05$.

DISCUSSION

The major issue in soft tissue augmentation is the rapid generation of highly stable adipose tissues or adipose tissue substitutes with sufficient volume at the site of soft tissue defects. From this viewpoint, it still seems advantageous to transplant autologous adipocyte-rich tissues in clinical settings in spite of advances in adipose tissue engineering that enable the development of adipose tissues at a slow rate.

The omentum is highly vascularized with microvascular ECs[21,22] and is composed mainly of adipocytes that produce a high level of VEGF.[23,27] It is expected that a massive amount of supplied ECs and the potent angiogenic factor, VEGF, synergistically facilitate revascularization when fragmented omentum tissues are transplanted. In addition, the omentum exists in a relatively easily accessible intraabdominal structure, and its removal does not result in any functional deficit.[21] Few studies have been performed on the use of the omentum as a free graft for soft tissue augmentation. Das *et al.* reported a preliminary study in which rabbit free omentum was transplanted under the rabbit scalp and dorsal skin by surgical placement,[32] but no further study has been reported.

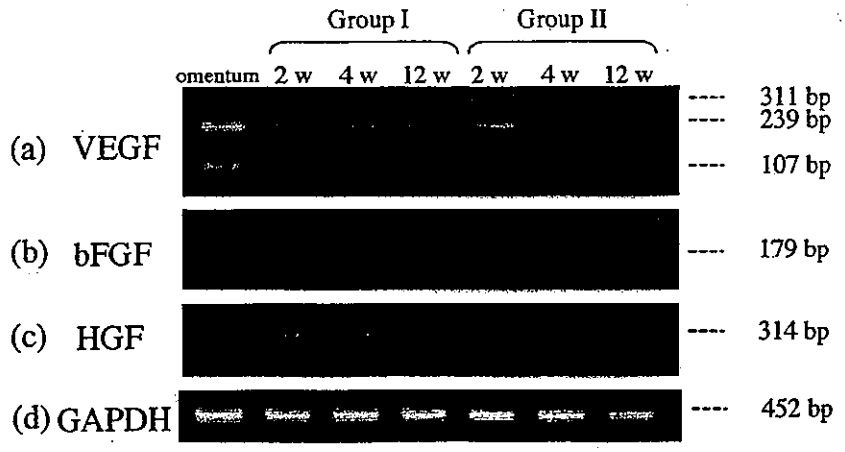

FIG. 8. Time-dependent changes in VEGF, bFGF, and HGF mRNA expression in transplanted tissues.

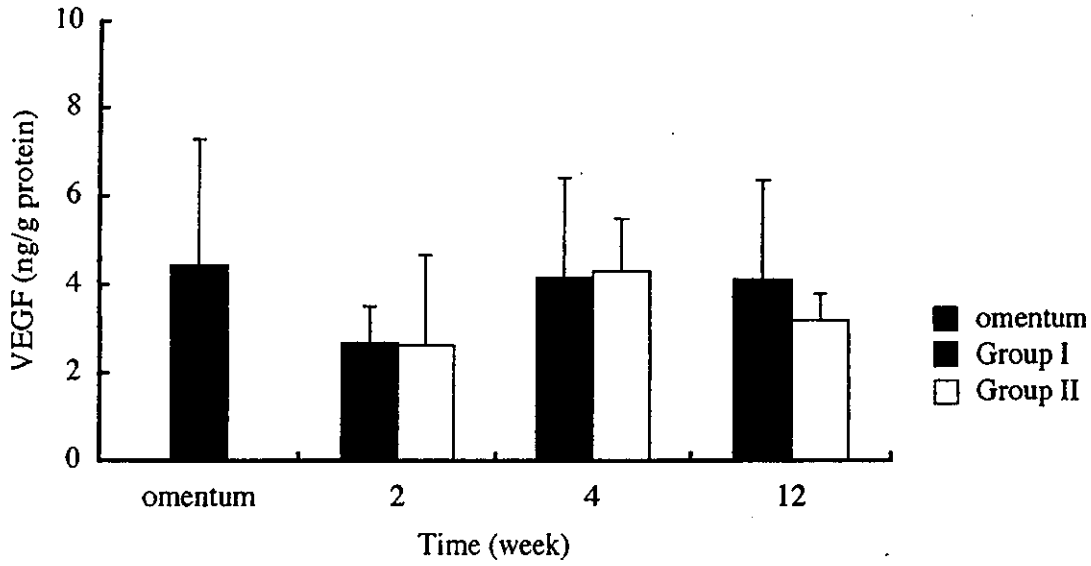

FIG. 9. Time-dependent changes in VEGF production in transplanted tissues (group I, solid columns; group II, open columns; each, $n = 5$). VEGF was not detected in the surrounding tissue to be transplanted.

This study was designed to determine the potential usefulness of the transplantation of fragmented omentum tissues or cotransplantation with preadipocytes in soft tissue augmentation. The transplanted tissues were evaluated in terms of gross appearance, weight change, tissue morphogenesis, and expression of angiogenic factors at the protein and genetic levels. The results are summarized as follows.

1. At 12 weeks postoperation, the transplanted tissue with minimal necrosis existed as a large mass (Fig. 2) and the weight losses of the transplanted tissues were limited to approximately 40% for group II (Table 1). Continuous weight losses among the transplanted tissues were noticed for group II (Table 1). On the other hand, although the initial loss of tissue in group I at the early transplantation period was noted to be similar to that in group II, such weight loss was not observed after 4 weeks of transplantation. There was a significant difference in weight loss between groups I and II at 12 weeks after transplantation. The reduced tissue loss observed for group I may be due to reduced necrosis and proliferation of preadipocytes and differentiation into mature adipocytes.

2. Extensive infiltration of inflammatory cells around the viable fragmented omentum tissues was observed at 2 weeks postoperation, followed by significant reduction in infiltration of inflammatory cells. The transplanted tissues were composed mainly of viable adipocytes and some pseudocysts surrounded by fibrotic septa at 12 weeks postoperation (Figs. 3 and 4).

3. The number of proliferating cells, which markedly exceeded that of apoptotic cells in the transplanted tissues, increased significantly during the early phase of transplantation (Fig. 6). It is presumed that the weight loss is due mainly to necrosis during the early phase of transplantation.

4. The TG content of the transplanted tissues was high compared with that of the surrounding tissue (almost 15-fold higher) for both groups I and II. These results sug-

TABLE 1. TIME-DEPENDENT CHANGES IN WEIGHT OF TRANSPLANTED TISSUES[a]

Group	*Transplanted tissues (mg)*	*Transplanted cells ($\times 10^6$)*	*Transplantation period (week)*[b]		
			2	*4*	*12*
I	524.5 ± 42.8	2.3 ± 1.4	85.9 ± 16.3	68.6 ± 21.8	71.1 ± 24.0
II	501.2 ± 55.4	—	84.5 ± 18.3	70.7 ± 15.8	59.9 ± 16.0[c]

[a]Weight percent relative to the initially transplanted tissues.
[b]$n = 5$ for each group and transplantation period.
[c]$p < 0.05$.

gest that addition of preadipocytes enhances the TG content of adipose constructs, which is probably due to differentiation of the transplanted preadipocytes into mature adipocytes (Fig. 7).

5. The capillary density of the transplanted tissues (approximately 65 capillaries/mm^2) decreased significantly to approximately 60% of that of omentum tissue at 2 weeks postoperation in groups I and II, but increased to the level of omentum tissue at 4 weeks postoperation (Fig. 5). The initial decrease in capillary density may be due to the acute necrosis of fragmented omentum tissues that failed to revascularize as the transplanted cells underwent more passive cellular necrosis rather than death by an active apoptotic process (Fig. 6).

6. VEGF mRNA expression and high VEGF production were observed throughout the transplantation period. HGF protein and bFGF protein were not detected, although the mRNAs for both growth factors were detected throughout the transplantation period (Figs. 8 and 9). These findings suggest that VEGF is the major factor contributing to the revascularization and angiogenesis of the transplanted tissues.

From this study it appears that the transplanted fragmented omentum tissues can survive as a free graft at least during the subacute phase (3 months) after transplantation. With this method, acute volumetric gains were noted right after transplantation and were maintained throughout the transplantation period; such gains cannot be obtained by previously reported methods of soft tissue augmentation based on tissue engineering. In addition, fragmented omentum tissues cotransplanted with preadipocytes have a better chance of forming a volumetric mass with a high triacylglycerol content. The advantage of using omentum tissue for soft tissue augmentation is that transplanted omentum tissues produce VEGF continuously after transplantation, which is greatly beneficial for revascularization and angiogenesis of the transplanted tissues. Das *et al.* reported that the mean survival of omentum grafts (not fragmented) at 3 months was 80 to 88%, as expressed in terms of weights of the surviving omentum compared with initial graft weight. However, they also reported that some amount of central necrosis was observed in the graft. Our results showed that there was no obvious central necrosis, indicating that fragmented omentum had a better chance of rapid revascularization for tissue survival compared with nonfragmented omentum tissue. This rapid revascularization and angiogenesis potential of fragmented omentum tissue also seem to play a substantial role in the survival and differentiation of preadipocytes when they are cotransplanted with omentum tissues. A major drawback of using omentum tissue is that a laparotomy is inevitable for harvesting the tissue. However, advances in laparoscopic surgery have enabled the harvesting of ometum with minimal invasion.[30,38] It is envisaged that optimization of the amount of fragmented omentum tissue and preadipocytes for transplantation and minimally invasive endoscopic harvesting of omentum tissues[38,39] may enable the realization of soft tissue augmentation in clinical settings; however, further longer term study, focusing on how to maintain the volumetric mass of fragmented omentum tissue–preadipocyte mixtures, must be done before clinical application.

ACKNOWLEDGMENT

This study was financially supported in part by a Grant-in-Aid for Scientific Research (A2-15200038) from the MEXT of Japan.

REFERENCES

1. Billings, E., Jr., and May, J.W., Jr. Historical review and present status of free fat graft autotransplantation in plastic and reconstructive surgery. Plast. Reconstr. Surg. **83,** 368, 1989.
2. Kononas, T.C., Bucky, L.P., Hurley, C., and May, J.W., Jr. The fate of suctioned and surgically removed fat after reimplantation for soft-tissue augmentation: A volumetric and histologic study in the rabbit. Plast. Reconstr. Surg. **91,** 763, 1993.
3. Fagrell, D., Enestrom, S., Berggren, A., and Kniola, B. Fat cylinder transplantation: An experimental comparative study of three different kinds of fat transplants. Plast. Reconstr. Surg. **98,** 90, 1996.
4. Nishimura, T., Hashimoto, H., Nakanishi, I., and Furukawa, M. Microvascular angiogenesis and apoptosis in the survival of free fat grafts. Laryngoscope **110,** 1333, 2000.
5. Chajchir, A. Fat injection: Long-term follow-up. Aesthetic Plast. Surg. **20,** 291, 1996.
6. Smahel, J. Experimental implantation of adipose tissue fragments. Br. J. Plast. Surg. **42,** 207, 1989.
7. Nguyen, A., Pasyk, K.A., Bouvier, T.N., Hassett, C.A., and Argenta, L.C. Comparative study of survival of autologous adipose tissue taken and transplanted by different techniques. Plast. Reconstr. Surg. **85,** 378, 1990.
8. Boschert, M.T., Beckert, B.W., Puckett, C.L., and Concannon, M.J. Analysis of lipocyte viability after liposuction. Plast. Reconstr. Surg. **109,** 761, 2002.
9. Robinson, J.K., and Hanke, C. W. Injectable collagen implant: Histopathologic identification and longevity of correction. J. Dermatol. Surg. Oncol. **11,** 124, 1985.
10. Elson, M. L. Soft tissue augmentation. Dermatol. Surg. **21,** 491, 1995.
11. Green, H., and Kehinde, O. Formation of normally differentiated subcutaneous fat pads by an established preadipose cell line. J. Cell. Physiol. **101,** 169, 1979.
12. Patrick, C.W., Jr., Chauvin, P.B., Hobley, J., and Reece, G.P. Preadipocyte seeded PLGA scaffolds for adipose tissue engineering. Tissue Eng. **5,** 139, 1999.

13. Schoeller, T., Lille, S., Wechselberger, G., Otto, A., Mowlawi, A., and Piza-Katzer, H. Histomorphologic and volumetric analysis of implanted autologous preadipocyte cultures suspended in fibrin glue: A potential new source for tissue augmentation. Aesthetic Plast. Surg. **25,** 57, 2001.
14. von Heimburg, D., Zachariah, S., Heschel, I., *et al.* Human preadipocytes seeded on freeze-dried collagen scaffolds investigated *in vitro* and *in vivo*. Biomaterials **22,** 429, 2001.
15. Halberstadt, C., Austin, C., Rowley, J., *et al.* A hydrogel material for plastic and reconstructive applications injected into the subcutaneous space of a sheep. Tissue Eng. **8,** 309, 2002.
16. Katz, A.J., Llull, R., Hedrick, M.H., and Futrell, J.W. Emerging approaches to the tissue engineering of fat. Clin. Plast. Surg. **26,** 587, 1999.
17. Kawaguchi, N., Toriyama, K., Nicodemou-Lena, E., Inou, K., Torii, S., and Kitagawa, Y. *De novo* adipogenesis in mice at the site of injection of basement membrane and basic fibroblast growth factor. Proc. Natl. Acad. Sci. U.S.A. **95,** 1062, 1998.
18. Tabata, Y., Miyao, M., Inamoto, T., *et al. De novo* formation of adipose tissue by controlled release of basic fibroblast growth factor. Tissue Eng. **6,** 279, 2000.
19. Yuksel, E., Weinfeld, A.B., Cleek, R., *et al. De novo* adipose tissue generation through long-term, local delivery of insulin and insulin-like growth factor-1 by PLGA/PEG microspheres in an *in vivo* rat model: A novel concept and capability. Plast. Reconstr. Surg. **105,** 1721, 2000.
20. Masuda, T., Furue, M., and Matsuda, T. Photocured-styrenated-gelatin microspheres for *de novo* adipogenesis through co-release of basic fibroblast growth factor, insulin, and insulin-like growth factor-1. Tissue Eng. **10,** 523, 2004.
21. Liebermann-Meffert, D. The greater omentum: Anatomy, embryology, and surgical applications. Surg. Clin. North Am. **80,** 275, 2000.
22. Chung-Welch, N., Patton, W.F., Shepro, D., and Cambria, R.P. Human omental microvascular endothelial and mesothelial cells: Characterization of two distinct mesodermally derived epithelial cells. Microvasc. Res. **54,** 108, 1997.
23. Goldsmith, H.S., Griffith, A.L., Kupferman, A., and Catsimpoolas, N. Lipid angiogenic factor from omentum. JAMA **252,** 2034, 1984.
24. Goldsmith, H.S., and Sax, D.S. Omental transposition for cerebral infarction: A 13-year follow-up study. Surg. Neurol. **51,** 342, 1999.
25. Vineberg, A. The bloodless greater omentum for myocardial revascularization. Dis. Chest **54,** 315, 1968.
26. Casten, D.F., and Alday, E.S. Omental transfer for revascularization of the extremities. Surg. Gynecol. Obstet. **132,** 301, 1971.
27. Zhang, Q.X., Magovern, C.J., Mack, C.A., Budenbender, K.T., Ko, W., and Rosengart, T.K. Vascular endothelial growth factor is the major angiogenic factor in omentum: Mechanism of the omentum-mediated angiogenesis. J. Surg. Res. **67,** 147, 1997.
28. McColl, I Reconstruction of the breast with omentum after subcutaneous mastectomy. Lancet **8108,** 134, 1979.
29. Walkinshaw, M., Caffee, H.H., and Wolfe, S.A. Vascularized omentum for facial contour restoration. Ann. Plast. Surg. **10,** 292, 1983.
30. Cothier-Savey, I., Tamtawi, B., Dohnt, F., Raulo, Y., and Baruch, J. Immediate breast reconstruction using a laparoscopically harvested omental flap. Plast. Reconstr. Surg. **107,** 1156, 2001.
31. Losken, A., Carlson, G.W., Culbertson, J.H., Hultman, C.S., Kumar, A.V., Jones, G.E., Bostwick, J., III, and Jurkiewicz, M.J. Omental free flap reconstruction in complex head and neck deformities. Head Neck **24,** 326, 2002.
32. Das, S.K., Cragun, J.R., Wheeler, E.S., Goshgarian, G., and Miller, T.A. Free grafting of the omentum for soft-tissue augmentation: A preliminary laboratory study. Plast. Reconstr. Surg. **68,** 556, 1981.
33. Gregoire, F., Genart, C., Hauser, N., and Remacle, C. Glucocorticoids induce a drastic inhibition of proliferation and stimulate differentiation of adult rat fat cell precursors. Exp. Cell Res. **196,** 270, 1991.
34. Hutley, L.J., Herington, A.C., Shurety, W., Cheung, C., Vesey, D.A., Cameron, D.P., and Prins, J.B. Human adipose tissue endothelial cells promote preadipocyte proliferation. Am. J. Physiol. Endocrinol. Metab. **281,** E1037, 2001.
35. Inoue, K., Sakurada, Y., Murakami, M., Shirota, M., and Shirota, K. Detection of gene expression of vascular endothelial growth factor and Flk-1 in the renal glomeruli of the normal rat kidney using the laser microdissection system. Virchows Arch. **442,** 159, 2003.
36. Casson, R.J., Wood, J.P., Melena, J., Chidlow, G., and Osborne, N.N. The effect of ischemic preconditioning on light-induced photoreceptor injury. Invest. Ophthalmol. Vis. Sci. **44,** 1348, 2003.
37. Shimazaki, K., Yoshida, K., Hirose, Y., Ishimori, H., Katayama, M., and Kawase, T. Cytokines regulate c-Met expression in cultured astrocytes. Brain Res. **962,** 105, 2003.
38. Saltz, R., Stowers, R., Smith, M., and Gadacz, T.R. Laparoscopically harvested omental free flap to cover a large soft tissue defect. Ann. Surg. **217,** 542, 1993.
39. Faga, A., Valdatta, L., Mezzetti, M., Buoro, M., and Thione, A. Ultrasound-assisted lipolysis of the omentum in dwarf pigs. Aesthetic Plast. Surg. **26,** 193, 2002.

Address reprint request to:
Takehisa Matsuda, Ph.D.
Department of Biomedical Engineering
Graduate School of Medical Sciences
Kyushu University
3-1-1 Maidashi, Higashiku
Fukuoka 812-8582, Japan

E-mail: matsuda@med.kyushu-u.ac.jp

Extracorporeal Cardiac Shock Wave Therapy Markedly Ameliorates Ischemia-Induced Myocardial Dysfunction in Pigs in Vivo

Takahiro Nishida, MD; Hiroaki Shimokawa, MD; Keiji Oi, MD; Hideki Tatewaki, MD; Toyokazu Uwatoku, MD; Kohtaro Abe, MD; Yasuharu Matsumoto, MD; Noriyoshi Kajihara, MD; Masataka Eto, MD; Takehisa Matsuda, PhD; Hisataka Yasui, MD; Akira Takeshita, MD; Kenji Sunagawa, MD

Background—Prognosis of ischemic cardiomyopathy still remains poor because of the lack of effective treatments. To develop a noninvasive therapy for the disorder, we examined the in vitro and vivo effects of extracorporeal shock wave (SW) that could enhance angiogenesis.

Methods and Results—SW treatment applied to cultured human umbilical vein endothelial cells significantly upregulated mRNA expression of vascular endothelial growth factor and its receptor Flt-1 in vitro. A porcine model of chronic myocardial ischemia was made by placing an ameroid constrictor at the proximal segment of the left circumflex coronary artery, which gradually induced a total occlusion of the artery with sustained myocardial dysfunction but without myocardial infarction in 4 weeks. Thereafter, extracorporeal SW therapy to the ischemic myocardial region (200 shots/spot for 9 spots at 0.09 mJ/mm^2) was performed (n=8), which induced a complete recovery of left ventricular ejection fraction (51±2% to 62±2%), wall thickening fraction (13±3% to 30±3%), and regional myocardial blood flow (1.0±0.2 to 1.4±0.3 $mL \cdot min^{-1} \cdot g^{-1}$) of the ischemic region in 4 weeks (all $P<0.01$). By contrast, animals that did not receive the therapy (n=8) had sustained myocardial dysfunction (left ventricular ejection fraction, 48±3% to 48±1%; wall thickening fraction, 13±2% to 9±2%) and regional myocardial blood flow (1.0±0.3 to 0.6±0.1 $mL \cdot min^{-1} \cdot g^{-1}$). Neither arrhythmias nor other complications were observed during or after the treatment. SW treatment of the ischemic myocardium significantly upregulated vascular endothelial growth factor expression in vivo.

Conclusions—These results suggest that extracorporeal cardiac SW therapy is an effective and noninvasive therapeutic strategy for ischemic heart disease. (***Circulation.* 2004;110:3055-3061.**)

Key Words: angiogenesis ■ contractility ■ hibernation ■ ischemia ■ regional blood flow

Prognosis of ischemic cardiomyopathy without an indication for coronary intervention or coronary artery bypass grafting still remains poor because medication is the only therapy to treat the disorder.[1] Thus, it is imperative that an effective and noninvasive therapy for ischemic cardiomyopathy be developed. Although no medication or procedure used clinically has shown efficacy in replacing myocardial scar with functioning contractile tissue, it could be possible to improve the contractility of the hibernating myocardium by inducing angiogenesis.

It recently has been suggested that shock wave (SW) could enhance angiogenesis in vitro.[2] SW is a longitudinal acoustic wave, traveling with the speed in water of ultrasound through body tissue. It is a single pressure pulse with a short needle-like positive spike <1 μs in duration and up to 100 MPa in amplitude, followed by a tensile part of several microseconds with lower amplitude.[3] SW is known to exert the "cavitation effect" (a micrometer-sized violent collapse of bubbles inside and outside the cells)[3] and recently has been demonstrated to induce localized stress on cell membranes that resembles shear stress.[4] If SW-induced angiogenesis could be reproduced in vivo, it would provide a unique opportunity to develop a new angiogenic therapy that would not require invasive procedures such as open-chest surgery or catheter intervention. Therefore, the present study was designed to examine the possible beneficial effects of SW on ischemia-induced myocardial dysfunction in a porcine model of chronic myocardial ischemia in vivo.

Methods

This study was reviewed by the Committee on Ethics in Animal Experiments of Kyushu University and was carried out under the

Received May 5, 2003; de novo received June 2, 2004; accepted June 17, 2004.

From the Departments of Cardiovascular Surgery (T.N., H.T., N.K., M.E., H.Y.), Cardiovascular Medicine (K.O., H.S., T.U., K.A., Y.M., A.T., K.S.), and Biomedical Engineering (T.M.), and the 21st Century COE Program on Lifestyle-Related Diseases (H.S., T.M.), Kyushu University Graduate School of Medical Sciences, Fukuoka, Japan.

Correspondence to Hiroaki Shimokawa, MD, PhD, Department of Cardiovascular Medicine, Kyushu University Graduate School of Medical Sciences, 3-1-1 Maidashi, Higashi-ku, Fukuoka 812-8582, Japan. E-mail shimo@cardiol.med.kyushu-u.ac.jp

Circulation is available at http://www.circulationaha.org

DOI: 10.1161/01.CIR.0000148849.51177.97

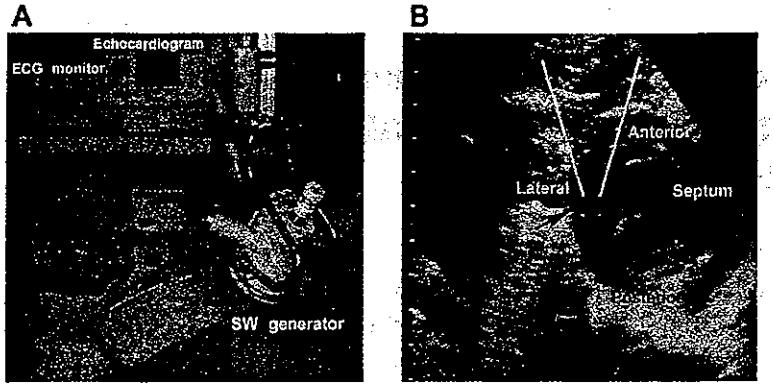

Figure 1. Extracorporeal cardiac SW therapy in action in a pig chronically instrumented with an ameroid constrictor. A, The machine is equipped with a SW generator and in-line echocardiography. The SW generator is attached to the chest wall when used. B, The SW pulse is easily focused on the ischemic myocardium under the guidance of echocardiography (black arrow).

Guidelines for Animal Experiments of Kyushu University and the Law (No. 105) and Notification (No. 6) of the Japanese Government.

Effect of SW on Human Umbilical Vein Endothelial Cells in Vitro

We purchased single-donor human umbilical vein endothelial cells (HUVECs) (Clonetics, Walkersville, Md) and cultured them in a complete endothelial medium (EBM-2 BulletKit, Clonetics). HUVECs were subcultured and used at passages 3 to 5 and were maintained in EBM-2. Twenty-four hours before the SW treatment, HUVECs (1×10^5) were resuspended in a 2-mL tube with EBM (Clonetics). We treated the HUVECs with 500 shots of SW at 4 different energy levels (0 [control], 0.02, 0.09, 0.18, and 0.35 mJ/mm^2) and stored them for 24 hours in the same medium before RNA extraction.

Ribonuclease Protection Assay

We analyzed equal amounts of mRNA by ribonuclease protection assay by means of the RiboQuant multiprobe template (PharMingen). Briefly, we hybridized RNA overnight with a ^{32}P-labeled RNA probe, which previously had been synthesized from the template set. We digested single-stranded RNA and free probe by ribonuclease A and T1. We then analyzed protected RNA on a 5% denaturing polyacrylamide gel. We analyzed several angiogenic factors, including vascular endothelial growth factor (VEGF) and its receptor, *fms*-like tyrosine kinase (Flt)-1, and angiopoietin and its receptor, tie-1, either by means of an NIH image or by means of autoradiography and subsequent quantification by densitometry (Alpha Innotech). For quantification, we normalized the signals for each sample of the blot with the corresponding signals of the housekeeping genes GAPDH and L32.

Porcine Model of Chronic Myocardial Ischemia

A total of 28 domestic pigs (25 to 30 kg in body weight) were used in this study. We anesthetized the animals with ketamine (15 mg/kg IM) and maintained anesthesia with an inhalation of 1.5% isoflurane for implantation of an ameroid constrictor, SW treatment, and euthanization. We opened the chest, suspended the pericardium and the left atrial appendage, revealed the left circumflex coronary artery (LCx), and put an ameroid constrictor around the proximal LCx to gradually induce a total occlusion of the artery in 4 weeks without causing myocardial infarction.[5,6] We also confirmed histologically that no myocardial necrosis had developed in the present porcine model (data not shown). This model is widely used to examine the effect of an angiogenic therapy in the ischemic hibernating myocardium.[5,6]

Extracorporeal Cardiac SW Therapy to Chronic Ischemic Myocardium

On the basis of the in vitro experiment, we applied a low energy of SW (0.09 mJ/mm2, ≈10% of the energy for the lithotripsy treatment) to 9 spots in the ischemic region (200 shots/spot) with the guidance of an echocardiogram equipped within a specially designed SW generator (Storz Medical AG) (Figure 1A). We were able to focus SW in any part of the heart under the guidance of echocardiography (Figure 1B). We applied SW to the ischemic myocardium in an R-wave–triggered manner to avoid ventricular arrhythmias. We performed the SW treatment (n=8) at 4 weeks after the implantation of an ameroid constrictor 3 times within 1 week, whereas animals in the control group (n=8) received the same anesthesia procedures 3 times a week but without the SW treatment. Because the SW treatment only requires the gentle compression of the generator to the chest wall, it is unlikely that this handling itself enhances angiogenesis in the ischemic myocardium.

Coronary Angiography and Left Ventriculography

After systemic heparinization (10 000 U/body), we performed coronary angiography and left ventriculography in a left oblique view with the use of a cineangiography system (Toshiba Medical). We semiquantitatively evaluated the extent of collateral flow to the LCx by the graded Rentrop score (0, no visible collateral vessels; 1, faint filling of side branches of the main epicardial vessel without filling the main vessel; 2, partial filling of the main epicardial vessel; 3, complete filling of the main vessel).[7] We also counted the number of visible coronary arteries in the LCx region. To compare the extent of collateral development at a given time, we selected the frame in which the whole left anterior descending coronary artery was first visualized.

Echocardiographic Evaluation

We performed epicardial echocardiographic studies at ameroid implantation (baseline) and at 4 and 8 weeks after the implantation of the constrictor (Sonos 5500, Agilent Technology). We calculated wall thickening fraction (WTF) by using the following formula: WTF = 100 × (end-systolic wall thickness − end-diastolic wall thickness) /end-diastolic wall thickness. We measured WTF when pigs were sedated, with and without dobutamine loading (15 $\mu g \cdot kg^{-1} \cdot min^{-1}$). Dobutamine was infused continuously from the ear vein, and WTF was measured after the hemodynamic condition was stabilized (in ≈5 minutes).

Measurement of Regional Myocardial Blood Flow

We evaluated regional myocardial blood flow (RMBF) with colored microspheres (Dye-Trak, Triton Technology) at ameroid implantation (baseline) and at 4 and 8 weeks after implantation.[8] We injected microspheres through the left atrium and aspirated a reference arterial blood sample from the descending aorta at a constant rate of 20 mL/min for 60 seconds using a withdrawal pump. We extracted microspheres from the left ventricular (LV) wall and blood samples by potassium hydroxide digestion, extracted the dyes from the spheres with dimethylformamide (200 μL), and determined their concentrations by spectrophotometry.[8] We calculated myocardial blood flow ($mL \cdot min^{-1} \cdot g^{-1}$) of the endocardial and epicardial lateral LV wall (the LCx region).

Analysis of Cardiac Enzymes

We measured serum concentrations of cardiac troponin T and creatinine kinase (CK)–MB by using chemiluminescence immuno-

assay before the SW treatment and at 4, 5 (2 hours after the SW treatment), and 8 weeks after ameroid implantation.

Factor VIII Staining

We treated paraffin-embedded sections with a rabbit anti-factor VIII antibody (N1505, Dako, Copenhagen, Denmark). We counted the number of factor VIII–positive cells in the endocardial and epicardial wall in 10 fields of the LCx region in each heart at 400× magnification.

Real-Time Polymerase Chain Reaction

To examine the effect of SW treatment on the ischemic myocardium in vivo, the animals with an ameroid constrictor were euthanized 1 week after the SW treatment. Total RNA was isolated from rapidly frozen ischemic LV wall (LCx region) after 3 SW treatments and was reverse transcribed. Quantification of VEGF and its receptor Flt-1 was performed by amplification of cDNA with an ABI Prism 7000 real-time thermocycler.

Western Blot Analysis for VEGF

We performed Western blot analysis for VEGF. Western blot analysis for VEGF was performed with and without 3 SW treatments. Three sections from the ischemic LV wall (LCx region) were measured. The regions containing VEGF proteins were visualized by electrochemiluminescence Western blotting luminal reagent (Santa Cruz Biotechnology). The extent of the VEGF was normalized by that of β-actin.

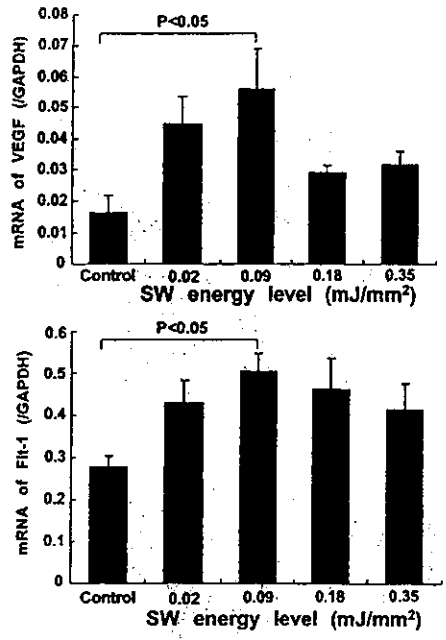

Figure 2. SW treatment upregulated mRNA expression of VEGF (A) and Flt-1 (B) in HUVECs in vitro with a maximum effect noted at 0.09 mJ/mm². Results are expressed as mean±SEM (n=10 each).

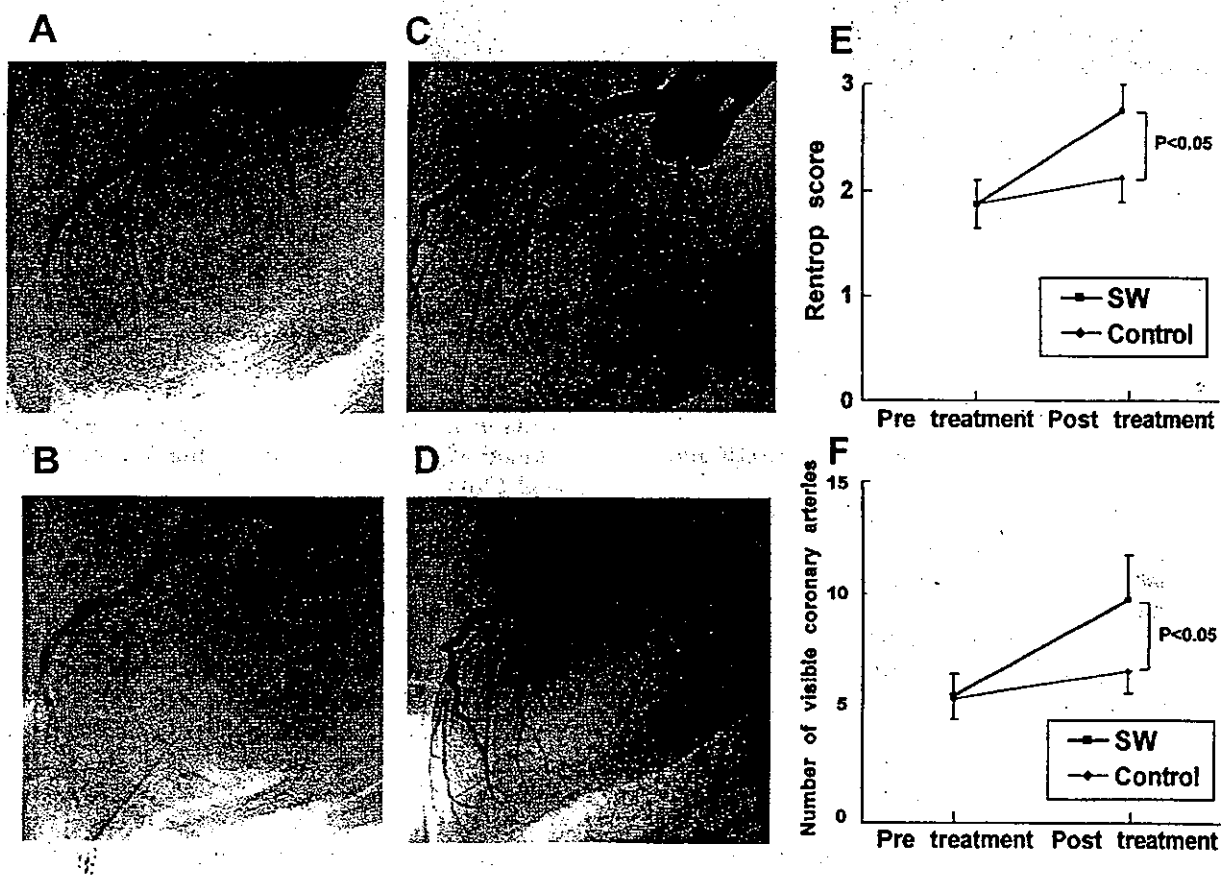

Figure 3. Extracorporeal cardiac SW therapy enhances coronary angiogenesis in vivo. A and C, Four weeks after the implantation of an ameroid constrictor, LCx was totally occluded and was perfused via collateral vessels with severe delay in both the control group (A) and the SW group (before SW therapy) (C). B and D, Four weeks after the first coronary angiography, no significant change in coronary vessels was noted in the control group (B), whereas a marked development of visible coronary vessels was noted in the SW group (D). E and F, Four weeks after the first coronary angiography, no significant increase in the Rentrop score (E) or visible coronary arteries from LCx (F) was noted in the control group, whereas increased Rentrop score and a marked development of visible coronary vessels were noted in the SW group. Results are expressed as mean±SEM (n=8 each).

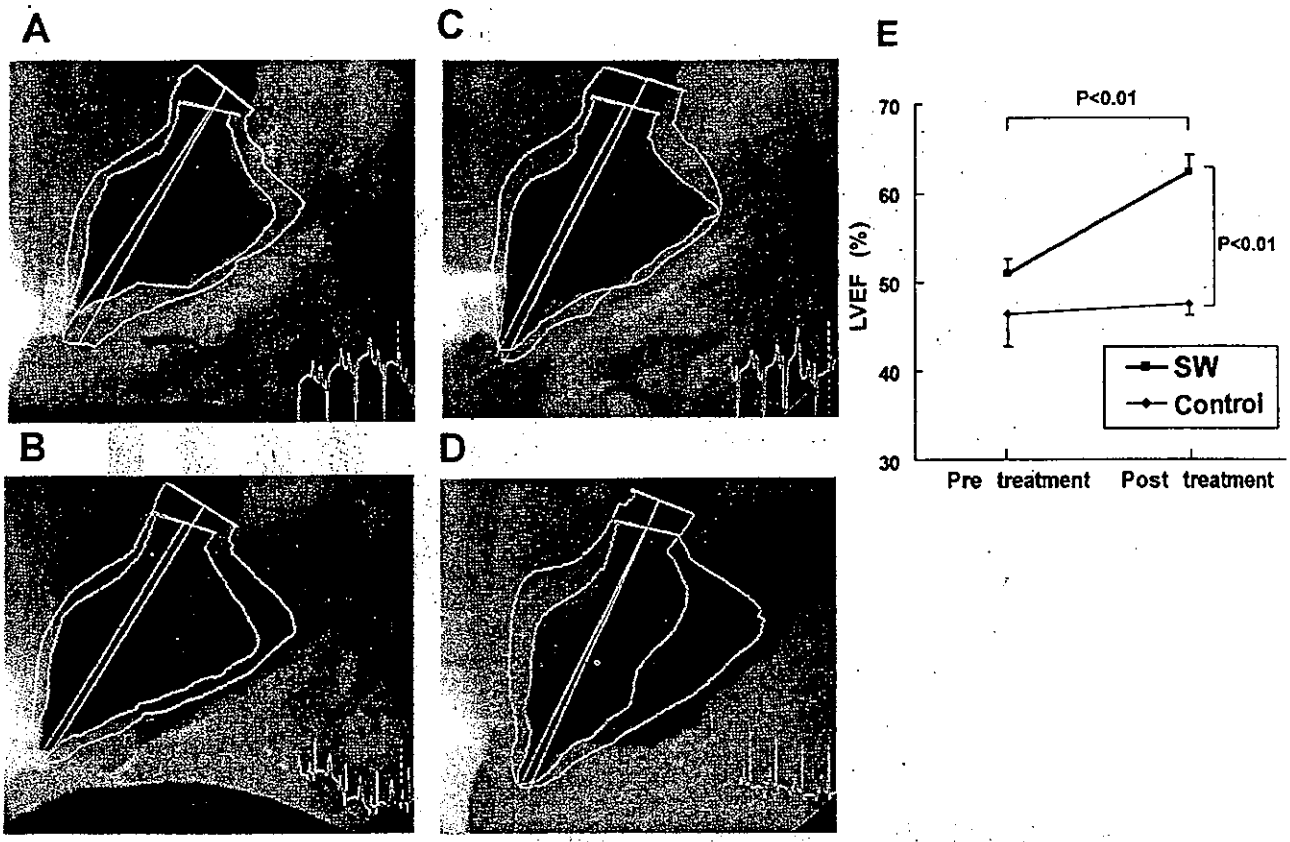

Figure 4. Extracorporeal cardiac SW therapy improves ischemia-induced myocardial dysfunction in vivo. A and C, Four weeks after the implantation of an ameroid constrictor, LV wall motion of the LCx (posterolateral) region was reduced in both the control (A) and the SW group (before the SW therapy) (C). B and D, Four weeks after the first left ventriculography, no significant change in LV wall motion was noted in the control group (B), whereas marked recovery was noted in the SW group (D). E, The SW therapy normalized left ventricular ejection fraction in the SW group but not in the control group. Results are expressed as mean±SEM (n=8 each).

Statistical Analysis

Results are expressed as mean±SEM. We determined statistical significance by analysis of variance for multiple comparisons. A value of $P<0.05$ was considered to be statistically significant.

Results

Effect of SW on mRNA Expression of VEGF and Flt-1 in HUVECs

SW treatment significantly upregulated mRNA expression of VEGF and its receptor Flt-1 in HUVECs, with a maximum effect noted at 0.09 mJ/mm^2 (Figure 2).

Effects of Extracorporeal Cardiac SW Therapy on Angiogenesis and Ischemia-Induced Myocardial Dysfunction

Four weeks after ameroid implantation, coronary angiography demonstrated a total occlusion of the LCx, which was perfused via collateral vessels with severe delay in both the control (Figure 3A) and the SW groups (Figure 3C). At 8 weeks after ameroid implantation (4 weeks after SW therapy), the SW group (Figure 3D), but not the control group (Figure 3B), had a marked development of coronary collateral vessels in the ischemic LCx region, an increased Rentrop score (Figure 3E), and an increased number of visible coronary arteries in the region (Figure 3F). Similarly, at 4 weeks, left ventriculography demonstrated an impaired left ventricular ejection fraction in both groups (Figure 4A, 4C, and 4E), whereas at 8 weeks, left ventricular ejection fraction was normalized in the SW group but remained impaired in the control group (Figure 4B, 4D, and 4E).

Effects of Extracorporeal Cardiac SW Therapy on Regional Myocardial Function and Myocardial Blood Flow

We serially measured WTF of the LCx region (lateral wall of the LV) by epicardiac echocardiography. At 4 weeks, we observed a significant reduction in WTF (%) in both groups (13±2 in the control group and 13±3 in the SW group; Figure 5A). At 8 weeks, however, the SW treatment markedly improved WTF in the SW group (30±3) but not in the control group (9±2) under control conditions (Figure 5A). Under dobutamine-loading conditions, which mimicked exercise conditions, WTF was further reduced at 4 weeks after the ameroid implantation in both groups (16±3 in the control and 18±2 in the SW groups), however, at 8 weeks, WTF was again markedly ameliorated only in the SW group (31±2) but not in the control group (16±4) (Figure 5B).

At 4 weeks, RMBF in the endocardium and epicardium (mL · min^{-1} · g^{-1}) was equally decreased in both groups (1.0±0.3 and 0.9±0.2 in the control group and 1.0±0.2 and 0.9±0.2 in the SW group, respectively). The SW treatment again improved RMBF in the endocardium (0.6±0.1 in the

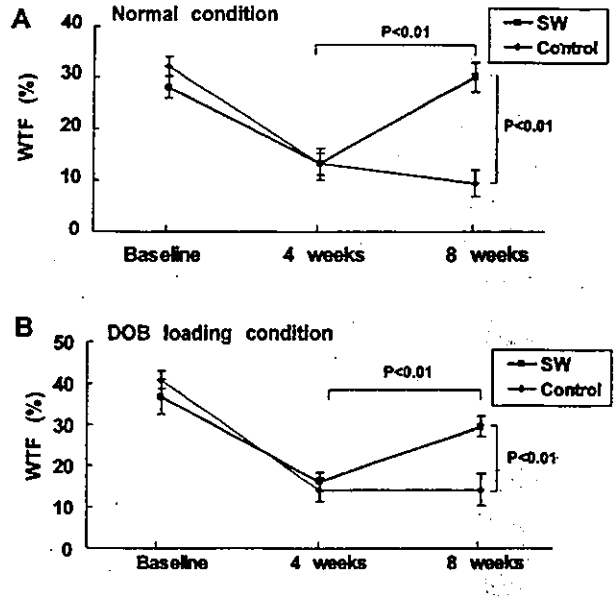

Figure 5. Extracorporeal cardiac SW therapy improves regional myocardial function in vivo. SW therapy induced a complete recovery of WTF of the ischemic lateral wall under control conditions (A) and under dobutamine (DOB) loading conditions (B). Results are expressed as mean±SEM (n=8 each).

control group and 1.4±0.3 in the SW group, $P<0.05$; Figure 6A) as well as in the epicardium (0.7±0.2 in the control group and 1.5±0.2 in the SW group, $P<0.05$; Figure 6B).

Effects of Extracorporeal Cardiac SW Therapy on Capillary Density and VEGF Expression in the Ischemic Myocardium

Factor VIII staining showed that the number of factor VIII–positive capillaries was increased in the SW group compared with the control group (Figure 7A and 7B). Quantitative analysis demonstrated that the number of capillaries was significantly higher in the SW group in both the endocardium (840±26 in the control group and 1280±45 in the SW group, $P<0.05$; Figure 7C) and the epicardium (820±30 in the control group and 1200±22 in the SW group, $P<0.05$; Figure 7D). RT-PCR analysis and Western blotting demonstrated a significant upregulation of VEGF mRNA expression (8.0±6 in the control group and 32±8 in the SW group, $P<0.05$; Figure 8A) and protein expression (2.23-fold increase in the SW groups, $P<0.05$; Figure 8B) after the SW treatment to the ischemic myocardium in vivo.

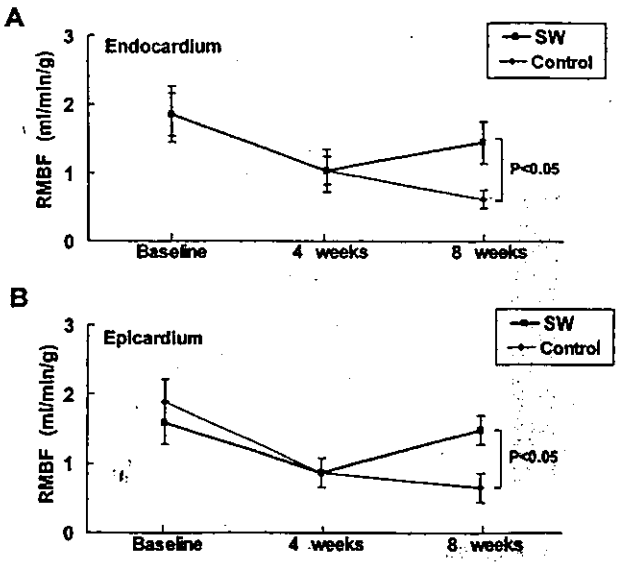

Figure 6. Extracorporeal cardiac SW therapy improves RMBF in vivo. SW therapy significantly increased RMBF, assessed by colored microspheres in both the endocardium (A) and the epicardium (B). Results are expressed as mean±SEM (n=8 each).

Side Effects of Extracorporeal Cardiac SW Therapy

All animals treated with the SW therapy were alive and showed no arrhythmias as assessed by 24-hour Holter ECG during and after the treatment (n=3; data not shown). There also was no myocardial cell damage as assessed by serum concentrations of CK-MB (ng/mL); the values before the SW treatment and at 4, 5 (2 hours after the SW treatment), and 8 weeks after the ameroid implantation were 5.0±0.6, 6.2±0.5, 5.5±0.2, and 7.1±0.9 in the control group and 5.1±0.2, 7.7±0.6, 6.1±0.6, and 6.4±0.4 in the SW group, respectively (n=6 each). The serum concentrations of troponin T were not detected in most cases in both groups. No significant differences were noted in hemodynamic variables (eg, heart rate or blood pressure) between the 2 groups (data not shown).

Discussion

The novel finding of the present study is that the extracorporeal cardiac SW therapy enhances angiogenesis in the ischemic myocardium and normalizes myocardial function in a porcine model of chronic myocardial ischemia in vivo. To the best of our knowledge, this is the first report that demonstrates the potential usefulness of extracorporeal cardiac SW therapy as a noninvasive treatment of chronic myocardial ischemia.

Extracorporeal Cardiac SW Therapy as a Novel Strategy for Ischemic Cardiomyopathy

Because of the poor prognosis of ischemic cardiomyopathy,[1,9] it is crucial to develop an alternative therapy for ischemia-induced myocardial dysfunction. To accomplish effective angiogenesis, it is mandatory to upregulate potent angiogenesis ligands, such as VEGF, and their receptors.[9,10] Furthermore, in the clinical setting, the goal for the treatment of ischemic cardiomyopathy should include not only enhancement of angiogenesis but also recovery of ischemia-induced myocardial dysfunction. In the present study, we were able to demonstrate that SW treatment (1) normalized global and regional myocardial functions as well as RMBF of the chronic ischemic region without any adverse effects in vivo, (2) increased vascular density in the SW-treated region, and (3) enhanced mRNA expression of VEGF and its receptor Flt-1 in HUVECs in vitro and VEGF production in the ischemic myocardium in vivo. Thus, SW-induced upregulation of the endogenous angiogenic system may offer a novel and promising noninvasive strategy for the treatment of ischemic heart disease.

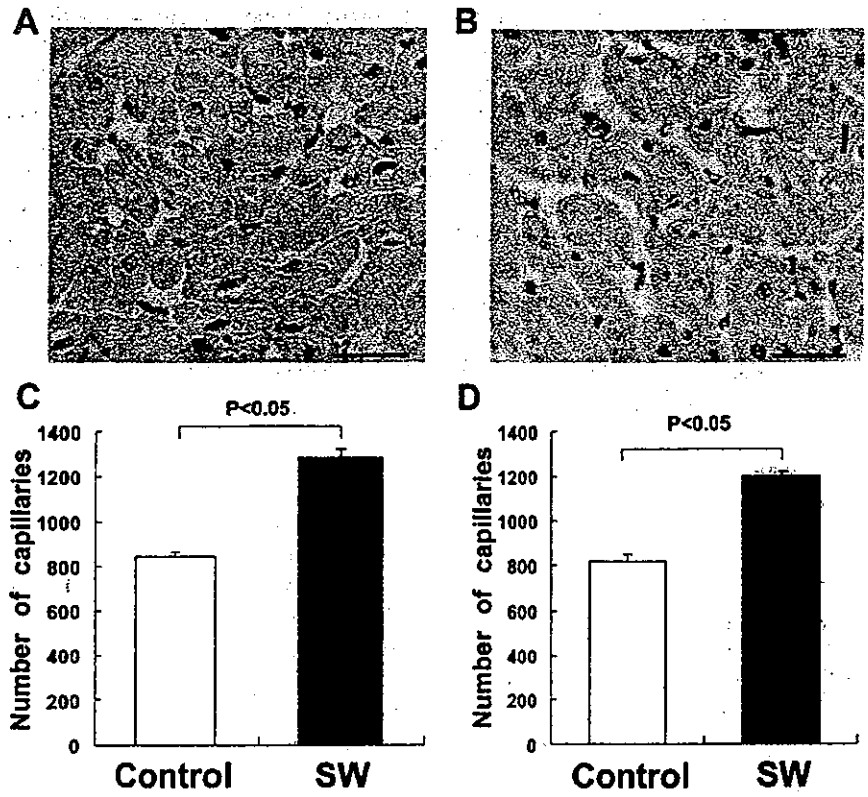

Figure 7. Extracorporeal cardiac SW therapy increases the density of factor VIII–positive capillaries in the ischemic myocardium. A and B, Factor VIII staining of the LCx region from the control (A) and the SW group (B). Scale bar represents 20 μm. C and D, Capillary density was significantly greater in the SW group (SW) than in the control group (Control) in both the endocardium (C) and the epicardium (D). Results are expressed as mean±SEM (n=6 each).

Advantages of Extracorporeal Cardiac SW Therapy

Recent attempts to enhance angiogenesis in the ischemic organs include gene therapy and bone marrow cell transplantation therapy. The main purpose of gene therapy is to induce overexpression of a selected angiogenic ligand (eg, VEGF) that leads to angiogenesis in the ischemic region. Although phase 1 trials of gene transfer of plasmid DNA encoding VEGF demonstrated safety and clinical benefit for the treatment of ischemic limb and heart,[11–13] gene therapy for ischemic cardiomyopathy is still at a preclinical stage. Bone marrow cell transplantation therapy, which depends on adult stem cell plasticity, also may be a useful strategy for angiogenesis because endothelial progenitor cells could be isolated from circulating mononuclear cells in humans and could be shown to be incorporated into neovascularization.[14] However, the need for invasive delivery of those cells to the ischemic myocardium may severely limit its usefulness in clinical situations.

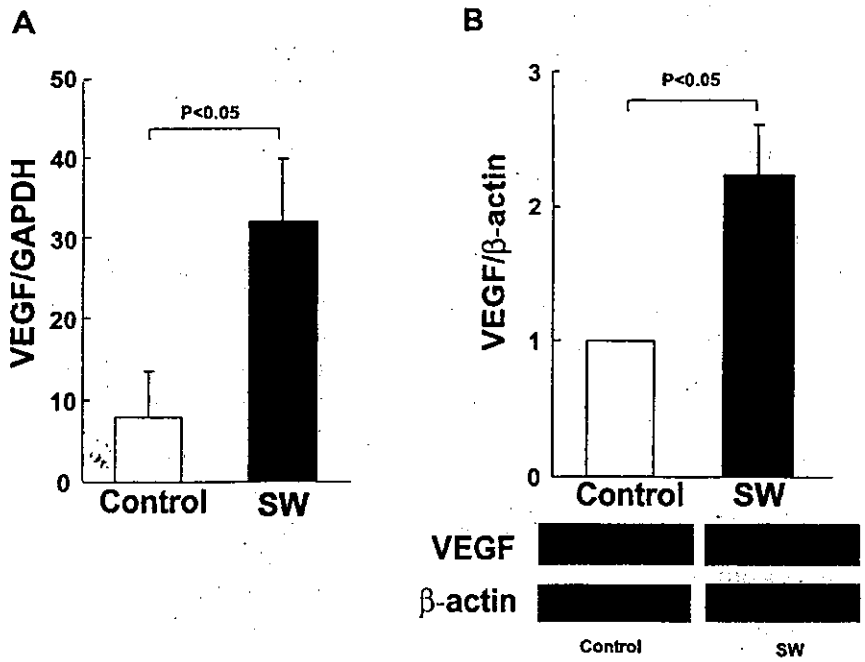

Figure 8. SW treatment upreglated mRNA (A) and protein (B) expression of VEGF in the ischemic myocardium (n=5 each).

A major advantage of the extracorporeal cardiac SW therapy over these 2 strategies is shown by the fact that it is quite noninvasive and safe, without any adverse effects. If necessary, we could repeatedly treat patients (even outpatients) with SW therapy because no surgery, anesthesia, or even catheter intervention is required for the treatment. This is an important factor in determining the clinical usefulness of angiogenic therapies in patients with ischemic cardiomyopathy. Thus, the extracorporeal cardiac SW therapy appears to be an applicable and noninvasive treatment for ischemic heart disease. Indeed, the SW treatment itself already has been clinically established as an effective and safe treatment for lithotripsy and chronic plantar fasciitis.[15,16] Our present results indicate that SW therapy, at ≈10% of the energy needed for lithotripsy treatment, is effective for in vivo angiogenesis in the ischemic heart.

Mechanisms for SW-Induced Angiogenesis

When a SW hits tissue, cavitation (a micrometer-sized violent collapse of bubbles) is induced by the first compression by the positive pressure part and the expansion with the tensile part of a SW.[3] Because the physical forces generated by cavitation are highly localized, SW could induce localized stress on cell membranes, as altered shear stress affects endothelial cells.[17] Recent reports have demonstrated the biochemical effects of SW, including hyperpolarization and Ras activation,[18] nonenzymatic nitric oxide synthesis,[19] and induction of stress fibers and intercellular gaps.[20] Although precise mechanisms for the SW-induced biochemical effects remain to be examined, these mechanisms may be involved in the underlying mechanisms for SW-induced angiogenesis. Indeed, Wang et al[21] reported that SW induces angiogenesis of the Achilles tendon–bone junction in dogs.

We were able to demonstrate that the SW treatment upregulated mRNA expression of VEGF and its receptor Flt in HUVECs in vitro and VEGF expression in the ischemic myocardium in vivo. Because the VEGF-Flt system is essential in initiating vasculogenesis and/or angiogenesis,[22] this effect of SW could explain, at least in part, the underlying mechanisms for SW-induced angiogenesis. It should be noted, however, that we showed only the upregulation of VEGF and Flt and that the effect of SW on signal transduction after receptor–ligand interaction still remains to be clarified. In addition, we need to fully elucidate the mechanisms for the SW-induced complete recovery of ischemia-induced myocardial dysfunction, although the increased myocardial blood flow caused by the SW treatment appears to play a primary role for the improved myocardial function. Further studies are required to determine the precise molecular mechanism for SW-induced angiogenesis and recovery of myocardial function.

In summary, we were able to demonstrate that noninvasive extracorporeal cardiac SW therapy effectively increases RMBF and normalizes ischemia-induced myocardial dysfunction without any adverse effects. Thus, extracorporeal cardiac SW therapy may be an effective, safe, and noninvasive therapy for ischemic cardiomyopathy.

Acknowledgments

This study was supported in part by a grant from the 21st Century COE Program and grants-in-aid from the Japanese Ministry of Education, Culture, Sports, Science, and Technology, Tokyo, Japan (Nos. 12032215, 12470158, 12877114, 13307024, 13557068), and the Japanese Ministry of Health, Labor, and Welfare, Tokyo, Japan. We thank Dr Ernest H. Marlinghaus, Storz Medical AG, Switzerland, for valuable discussion about our study, and Prof S. Mohri at the Center of Biomedical Research, Kyushu University Graduate School of Medical Sciences, for cooperation in this study.

References

1. Jessup M, Brozena S. Heart failure. *N Engl J Med.* 2003;348:2007–2018.
2. Gutersohn A, Caspari G. Shock waves upregulate vascular endothelial growth factor m-RNA in human umbilical vascular endothelial cells. *Circulation.* 2000;102(suppl):18.
3. Apfel RE. Acoustic cavitation: a possible consequence of biomedical uses of ultrasound. *Br J Cancer.* 1982;45(suppl):140–146.
4. Maisonhaute E, Prado C, White PC, et al. Surface acoustic cavitation understood via nanosecond electrochemistry, part III: shear stress in ultrasonic cleaning. *Ultrason Sonochem.* 2002;9:297–303.
5. O'Konski MS, White FC, Longhurst J, et al. Ameroid constriction of the proximal left circumflex coronary artery in swine: a model of limited coronary collateral circulation. *Am J Cardiovasc Pathol.* 1987;1:69–77.
6. Roth DM, Maruoka Y, Rogers J, et al. Development of coronary collateral circulation in left circumflex ameroid–occluded swine myocardium. *Am J Physiol.* 1987;253:H1279–1288.
7. Rentrop KP, Cohen M, Blanke H, et al. Changes in collateral channel filling immediately after controlled coronary artery occlusion by an angioplasty balloon in human subjects. *J Am Coll Cardiol.* 1985;5:587–592.
8. Prinzen FW, Bassingthwaighte JB. Blood flow distributions by microsphere deposition methods. *Cardiovasc Res.* 2000;45:13–21.
9. Carmeliet P, Ferreira V, Breier G, et al. Abnormal blood vessel development and lethality in embryos lacking a single VEGF allele. *Nature.* 1996;380:435–439.
10. Ferrara N, Carver-Moore K, Chen H, et al. Heterozygous embryonic lethality induced by targeted inactivation of the VEGF gene. *Nature.* 1996;380:439–442.
11. Isner JM, Pieczek A, Schainfeld R, et al. Clinical evidence of angiogenesis after arterial gene transfer of phVEGF165 in patient with ischaemic limb. *Lancet.* 1996;348:370–374.
12. Baumgartner I, Pieczek A, Manor O, et al. Constitutive expression of phVEGF165 after intramuscular gene transfer promotes collateral vessel development in patients with critical limb ischemia. *Circulation.* 1998;97:1114–1123.
13. Losordo DW, Vale PR, Symes JF, et al. Gene therapy for myocardial angiogenesis: initial clinical results with direct myocardial injection of phVEGF165 as sole therapy for myocardial ischemia. *Circulation.* 1998;98:2800–2804.
14. Asahara T, Murohara T, Sullivan A, et al. Isolation of putative progenitor endothelial cells for angiogenesis. *Science.* 1997;275:964–966.
15. Auge BK, Preminger GM. Update on shock wave lithotripsy technology. *Curr Opin Urol.* 2002;12:287–290.
16. Weil LS Jr, Roukis TS, Weil LS, et al. Extracorporeal shock wave therapy for the treatment of chronic plantar fasciitis: indications, protocol, intermediate results, and a comparison of results to fasciotomy. *J Foot Ankle Surg.* 2002;41:166–172.
17. Fisher AB, Chien S, Barakat AI, et al. Endothelial cellular response to altered shear stress. *Am J Physiol.* 2001;281:L529–L533.
18. Wang FS, Wang CJ, Huang HJ, et al. Physical shock wave mediates membrane hyperpolarization and Ras activation for osteogenesis in human bone marrow stromal cells. *Biochem Biophys Res Commun.* 2001;287:648–655.
19. Gotte G, Amelio E, Russo S, et al. Short-time non-enzymatic nitric oxide synthesis from L-arginine and hydrogen peroxide induced by shock waves treatment. *FEBS Lett.* 2002;520:153–155.
20. Seidl M, Steinbach P, Worle K, et al. Induction of stress fibres and intercellular gaps in human vascular endothelium by shock-waves. *Ultrasonics.* 1994;32:397–400.
21. Wang CJ, Huang HY, Pai CH. Shock wave–enhanced neovascularization at the tendon-bone junction: an experiment in dogs. *J Foot Ankle Surg.* 2002;41:16–22.
22. Millauer B, Wizigmann-Voos S, Schnurch H, et al. High affinity VEGF binding and developmental expression suggest Flk-1 as a major regulator of vasculogenesis and angiogenesis. *Cell.* 1993;72:835–846.